Modeling of Gasoline Direct Injection Mixture Formation Using KIVA-3V: Development of Spray Breakup & Wall Impingement Models and Validation with Optical Engine Planar Laser Induced Fluorescence Measurements.

*B. P. Vanzieleghem, C. A. Chryssakis, R. O. Grover, V. Sick, H. G. Im, and D. N. Assanis

W.E. Lay Automotive Laboratory
Department of Mechanical Engineering, University of Michigan
1231 Beal Ave., Ann Arbor, MI 48105, U.S.A.

Key Words: Gasoline, Injection, Modeling, Optical, Laser

ABSTRACT

The computational code KIVA-3V has been used as the modeling platform for Gasoline Direct Injection engine simulations. Improved models for fuel injection, wall impingement and stratified combustion have been implemented. To complement the modeling effort, experimental data of an optical engine has provided extensive data for validating the new models. The experimental data include Planar Laser Induced Fluorescence measurements, of the injection, mixing and combustion events in an optical engine. In this work, focus is given on fuel injection, wall impingement and air-fuel mixing.

INTRODUCTION

The design of more powerful, fuel-efficient, and environmentally friendly gasoline engines is currently one of the main goals of engine researchers. With the advent of increasingly stringent fuel consumption and emissions standards, engine manufacturers face the challenging task of delivering conventional vehicles that abide by these regulations. Many automotive manufacturers are responding to the challenge of developing highly efficient, Ultra Low Emission Vehicles (ULEV's) by developing Gasoline Direct Injection (GDI) systems [1-7]. Controlling the mixture formation of a GDI engine under a wide range of engine operating conditions is essential to reduce smoke and particulate generation and optimize fuel economy. A valuable tool for understanding and controlling the mixture formation is the combination of optical diagnostics with Computational Fluid Dynamics (CFD) simulations of the in-cylinder processes.

In order to perform reliable CFD simulations of a GDI engine, appropriate models for fuel injection, mixing and combustion are required. Accurate predictions of the air-fuel mixing process are critical in order to provide correct initial conditions for the combustion modeling. It is common practice to validate fuel injection and wall impingement models against experimental data acquired under constant temperature and pressure conditions, in constant-volume vessels (bombs). These experimental set-ups allow for highly accurate measurements with laser diagnostics methods and offer precious insight on the physical phenomena occurring during injection and wall impingement. However, in an engine environment, temperature and pressure conditions are continuously varying, presenting an additional challenge for the models. Therefore, it is important to validate these models against measurements acquired in optical engines configurations. Han et al. [8-9] have presented comparisons of optical measurements with spray evolution and fuel vapor distribution calculations for stratified operating conditions; however, there exists a void in the literature for this type of study at early injection timings. In the current work, focus is given on coupling the individual models for fuel injection, wall impingement and combustion and validate them under homogeneous engine operation, achieved by early fuel injection.

The submodels developed for fuel injection, spray breakup and wall impingement have been extensively validated against optical diagnostics experiments [10-13] and will be briefly described here. The validation was performed with data acquired under atmospheric conditions and should apply to early injection timings in a

GDI engine. Subsequently, comparison with Planar Laser Induced Fluorescence (PLIF) measurements from an optical single-cylinder engine will be presented to demonstrate the predictive capability of the models. In a later study, these models are coupled to a combustion model applicable for both stratified and homogeneous operation [14].

EXPERIMENTAL SETUP

The experimental setup consists of a single-cylinder, four stroke GDI engine with a four valve head, featuring full optical access, variable swirl [15] and dimensions as given in Table 1. The spark plug is located on the exhaust side of the combustion chamber, while the injector is located on the intake side. The optical access is achieved by a quartz window in both the piston and pent roof of the engine, combined with a quartz cylinder. The piston window is smaller than the engine bore, giving optical access to part of the engine's volume. The swirl is varied by restricting the airflow through one of the two intake valves.

Table 1: Optical Engine Geometry

Connecting Rod	159 mm
Bore	86 mm
Stroke	86 mm
Clearance Volume	49.9 cm^3
Displacement	499.15 cm^3
Compression Ratio	11.0
Optical Piston Window	55 mm
Intake Temperature	45^o C
Intake Pressure	45 kPA

A laser induced fluorescence (LIF) technique, with Toluene as a tracer added to the fuel (iso-octane), has been used to provide visualization of the fuel-injection, mixing and combustion processes [15]. The LIF signal was calibrated by taking images of early injection events 90^o after top-dead-center (ATDC), at which point the fuel had sufficient time to mix and evaporate to create a homogeneous, gaseous fuel-air mixture. Dependence of the toluene signal on fuel concentration, laser energy and gas temperature was corrected for in the measurements.

COMPUTATIONAL FRAMEWORK

For the numerical simulations performed in this work a modified version of the Los Alamos KIVA-3V code [17] has been used. The modifications include the fuel injection model, the wall impingement model and the Coherent Flame Combustion model [14]. The computational mesh consists of approximately 70,000 cells. An image of the grid showing the intake and exhaust ports is shown in Figure 1. The adopted mesh has been found to generate a swirl behavior very similar to that in the optical

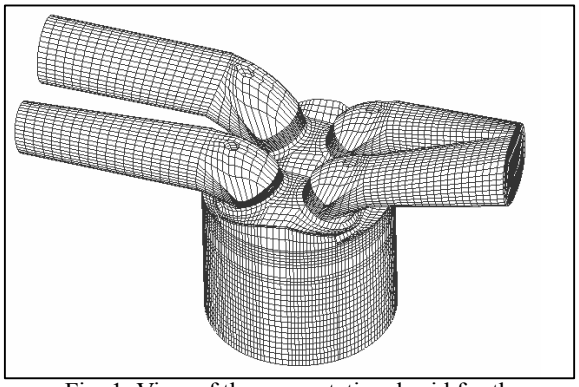

Fig. 1: View of the computational grid for the optical engine

engine. To generate the swirl, one of the valves is deactivated completely.

Fuel Injection Model

A comprehensive model for sprays emerging from high-pressure swirl injectors has been developed, accounting for both primary and secondary atomization [10-11]. The model considers the transient behavior of the pre-swirl spray and the steady-state behavior of the main spray. The pre-swirl spray modeling is based on an empirical solid-cone approach with varying cone angle. First, a solid-cone-like injection is performed, representing the pre-swirl spray. The cone angle is gradually increased, using a linear profile. At the transition point, the code switches into a hollow-cone structure, while the cone angle is still increasing, until the steady-state value is reached.

The primary breakup approach adopted here for the main spray is based on the Linearized Instability Sheet Atomization (LISA) model [17-18], with appropriate extensions to include a swirl velocity component. A Rosin-Rammler cumulative distribution is used for calculating the droplet size. For the secondary droplet breakup the TAB model [19] is being used both for the pre-swirl and the main spray, with its baseline constants.

Wall Impingement Model

A wall impingement model, developed by Grover et al. [12-13] has been used to improve the prediction capability of spray-wall interactions. The model conserves mass, tangential momentum and energy of an impinging parcel. This model focuses on spray impact on dry and wet surfaces below the fuel's Leidenfrost temperature, a scenario encountered under typical engine operating conditions [20].

Three splashing parcels and one wallfilm parcel are used to represent the shattering of a splashing droplet upon impact with the surface. It is assumed that the impulsive force on an impinging droplet normal to the surface is dominant allowing one to treat the magnitude of its tangential momentum component constant after impact. The viscous dissipation of an impinging droplet and kinetic energy of the wallfilm are accounted for in the energy conservation equation.

COMPARISON WITH EXPERIMENTS

Cylinder Charge Air Motion

Figure 2 shows the velocity field in a horizontal section 1 mm below the firing deck of the engine (the firing deck is defined as the location where the head and cylinder meet), at spark timing (340° CA). A more organized flow structure, with a counter-clockwise swirl, can be observed in the high swirl case. The low swirl case does not exhibit an obvious swirling motion, and the velocity magnitudes are slightly lower, shown by the shorter velocity vectors. The low and high swirl conditions correspond to experimentally measured swirl numbers of 0.8 and 5.5 respectively.

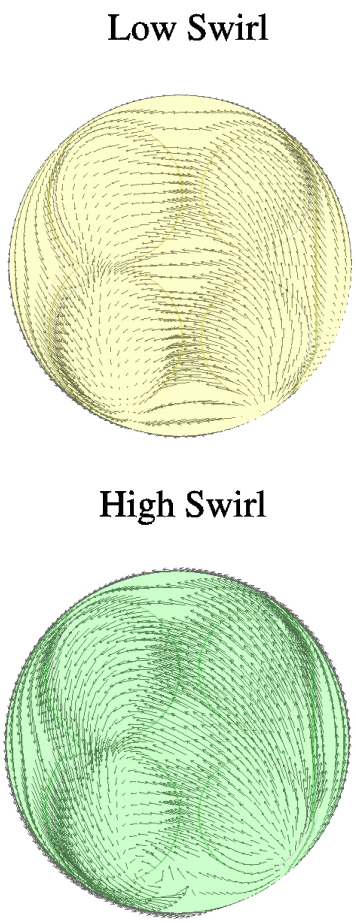

Fig. 2: Comparison of the velocity vectors for the low and high-swirl case, 2000 rpm (viewed from below, intake valves on left side, exhaust on right).

Fuel Injection Comparison

The fuel injection and mixing process were validated against LIF spray images and spray vaporization rates. The simulated and experimental results were in good agreement and lead us to believe that the boundary conditions were adequate for an assessment of the combustion model.

The spray images obtained with the LIF technique were taken at different horizontal planes. The plane chosen here for validation purposes is located eight millimeters below the firing deck, as seen in Figure 3. Figure 4 shows the comparison of the modeled spray and the experimental visualization on the same geometrical scale, for the 2000 rpm, low swirl case. The modeled spray shows both the equivalence ratio of the evaporated fuel and the fuel droplets in liquid form, while the experiment was setup to visualize the liquid core of the spray. It can be seen from the comparison that the liquid droplet distribution of the model is in good agreement with the observed spray from the experiments. The radius of the liquid spray corresponds to the spray radius observed in the experiments, and the timing of when the spray has passed the plane agrees with the experiments, as can be seen in the image for 97° CA. The experimental observation does suffer from an attenuation of the laser beam as the spray is being traversed. The gaseous fuel distribution seen in the model, however, is not observed in the experiments.

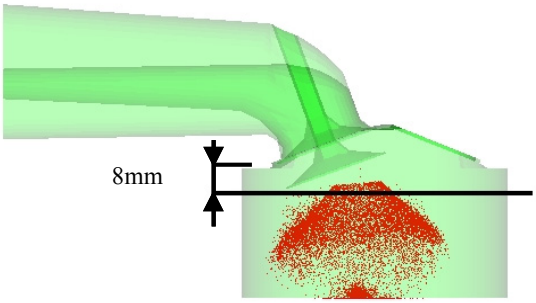

Fig. 3: Location of the laser sheet.

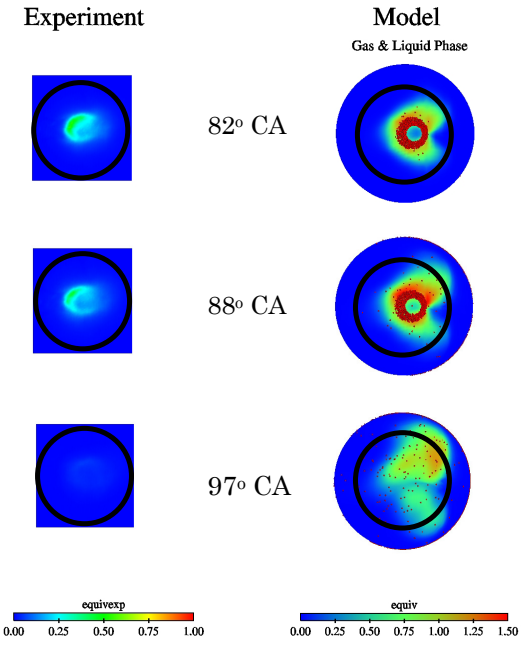

Fig. 4: Comparison of experimental and modeled spray, low swirl, 2000 rpm, crank angles 82° - 88°, during the intake stroke.

Aside from the above visual comparison of the simulation and the experiments, a number of the qualitative experimental observations were found to be reproduced in the simulation. For the 2000 rpm case, it was observed in the experiments that the spray evaporates faster for the high swirl operation [15]. In addition, the spray was shifted to the left of the cylinder geometry in the high swirl case at 2000 rpm. Furthermore, it was conjectured that rich regions should be present at the periphery of the cylinder, where optical access was not possible for the high swirl cases at both 600 and 2000 rpm. This conclusion was reached after spatially-averaging the equivalence ratio in a plane 1 mm above the firing deck, and achieving an equivalence ratio lower than one for the high swirl cases. Figure 5 shows the modeling prediction of the spray plume for the high and low swirl, 2000 rpm, operating point during the injection process. A careful observation of the images reveals that the spray is pulled to the intake side of the engine for the high swirl operation, consistent with the experimental observation. For the result at 94° CA, the spray hits the cylinder liner in a higher location for the high swirl case compared to the low swirl case. For the 600 rpm case, the difference between both sprays for the high and low swirl case was less pronounced, but the high swirl condition still shows a movement towards the intake side of the combustion chamber, as seen in Figure 6. Figures 7 and 8 show the evaporation rate of the droplets for the 600 and 2000 rpm cases. It is clear that for the 2000 rpm, high swirl case, the evaporation proceeds at a faster rate than for the low swirl case. For the 600 rpm operating point, the difference between the low and high swirl operation is less significant.

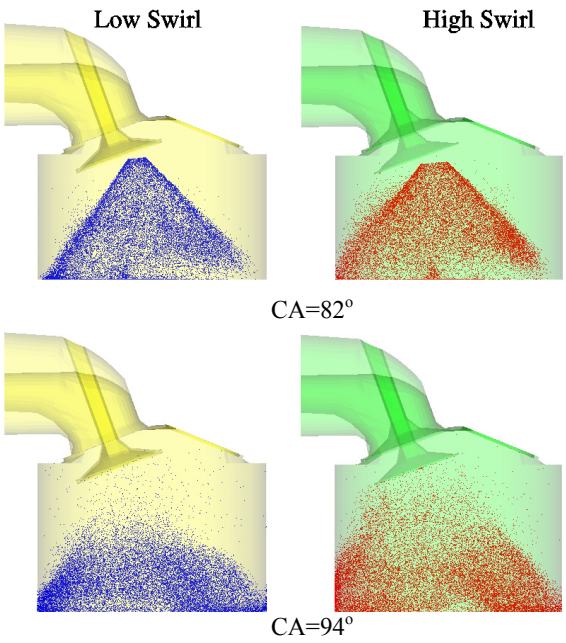

Fig. 5: Comparison of the modeled spray for the low and high swirl case at 2000 rpm.

When the experimental results for the fuel concentration were spatially averaged in the field of view plane 1 mm above the firing deck, the high swirl case, for both 600 and 2000 rpm, resulted in a leaner equivalence ratio [15]. Since the fueling was set to yield an overall equivalence ratio of 1.0, it was conjectured that rich regions had to be present elsewhere in the combustion chamber. Investigation of the other elevations did not reveal these rich regions, leading to the conclusion that rich areas must occur outside the field of view of the laser imaging, at the periphery of the cylinder where optical access was not possible. Figure 9 shows the fuel distribution at the time of spark, which corresponds to the timing of the experimental image that was spatially averaged to determine the overall equivalence ratio. From the images, it is clear that a significant amount of fuel can be found at the periphery of the combustion chamber for the high swirl case, which further supports the experimental observations.

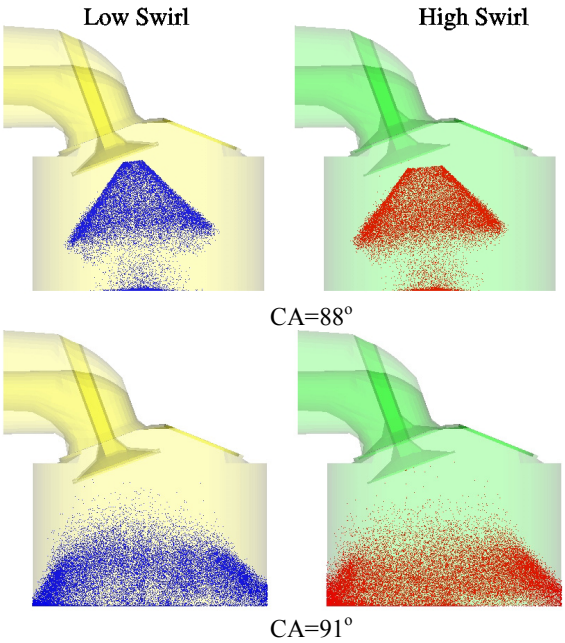

Fig. 6: Comparison of the modeled spray for the low and high swirl case at 600 rpm.

CONCLUSIONS

To accurately simulate GDI engine operation under homogeneous chare conditions, a set of computational models, including fuel injection, wall impingement and stratified combustion, has been developed and implemented in to KIVA-3V. To validate the results of the fuel injection and air-fuel mixing modeling, comparisons of all the engine processes were performed with experiments on a single-cylinder optical GDI engine. Agreement between the model and the experimental results was shown to be very good.

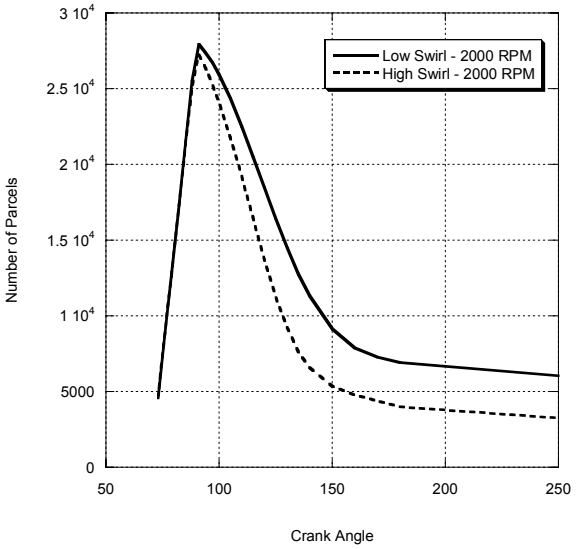

Fig. 7: Comparison of evaporation rate for the 2000 rpm low and high swirl cases.

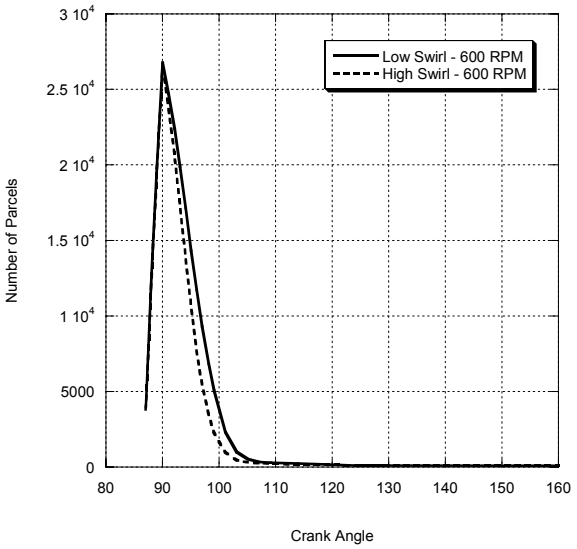

Fig. 8: Comparison of evaporation rate for the 600 rpm low and high swirl cases.

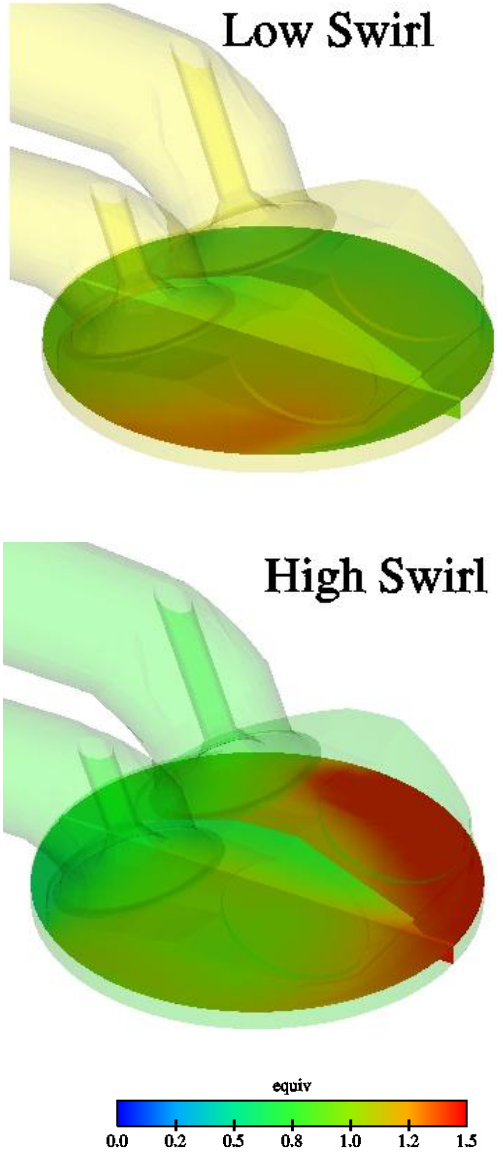

Fig. 9: Comparison of equivalence ratio distribution for the 2000 rpm low and high swirl cases.

REFERENCES

[1] Kume, T., Iwamoto, Y., Iida, K., Murakami, M., Akishino, K., and Ando, A., "Combustion Control Technologies for Direct Injection SI Engine", *SAE Paper* 960600, 1996

[2] Iwamoto, Y., Noma, K., Nakayama, O., Yamauchi, T., and Ando, H., "Development of Gasoline Direct Injection Engine", *SAE Paper* 970541, 1997

[3] Kuwahara, K., Ueda, K., and Ando, H., "Mixing control Strategy for Engine Performance Improvement in a Gasoline Direct Injection Engine", *SAE Paper* 980158, 1998

[4] Harada, J., Tomita, T., Mizuno, H., Mashiki, Z., and Ito, Y., "Development of Direct Injection Gasoline Engine", *SAE Paper* 970540, 1997

[5] Tomoda, T., Sasaki, S., Sawada, D., Saito, A., and Sami, H., "Development of Direct Injection Gasoline Engine - Study of Stratified Mixture Formation", *SAE Paper* 970539, 1997

[6] Wurms, R., Grigo, M., Hatz, W., "Audi FSI technology ~ Improved performance and reduced fuel consumption", *SAE Paper* 2002-33-002, 2002

[7] Borgmann, K., Liebl, J., Hofmann, R., Schausberger, C., Schwarzbauer, G., "The innovative V12 powertrain for the new 7 Series", *SAE Paper* 2003-08-0202, 2003

[8] Han Z., Xu Z., Wooldridge S., Yi J., Lavoie G., "Modeling of DISI Engine Sprays with Comparison to Experimental In-Cylinder Spray Images", *SAE Paper* 2001-01-3667, 2001

[9] Han Z., Weaver C., Wooldridge S., Alger T., Hilditch J., McGee J., Westrate B., Xu Z., Yi J., Chen X., Trigui N., Davis G., "Development of a New Light Stratified-Charge DISI Combustion System for a Family of Engines with Upfront CFD Coupling with Thermal and Optical Engine Experiments", *SAE Paper* 2004-01-0545, 2004

[10] Chryssakis, C. A., Driscoll, K. D., Sick, V. Assanis, D. N., "Validation of an Enhanced Liquid Sheet Atomisation Model Against Quantitative Laser Diagnostic Measurements", *18th Annual Conference on Liquid Atomization and Spray Systems*, Zaragoza, Spain, September 2002

[11] Chryssakis, C.A., Assanis, D. N., Lee, J., Nishida, K., "Fuel Spray Simulation of High-Pressure Swirl-Injector for DISI Engines and Comparison with Laser Diagnostic Measurements", SAE Paper 2003-01-0007, March 2003

[12] Grover, R.O., Assanis, D.N., "A Spray Wall Impingement Model Based Upon Conservation Principles," *Fifth International Symposium on Diagnostics and Modeling of Combustion in Internal Combustion Engines*, pp. 551-559, 2001

[13] Grover, R.O., Assanis, D.N., Lippert, A.M., El Tahry, S.H., Drake, M.C., Fansler T.D., Harrington D.L., "A Critical Analysis of Splash Criteria for GDI Spray Impingement", *15th Annual Conference on Liquid Atomization and Spray Systems*, Madison, WI, May 2002

[14] B.P. Vanzieleghem, V. Sick, H. G. Im and D.N. Assanis, "Modeling of Gasoline Direct Injection Combustion using KIVA-3V: Development of an Extended Coherent Flamelet Model and Validation with Optical Engine Planar Laser Induced Fluorescence Measurements", COMODIA 2004, Yokohama, Japan, August 2004

[15] Frieden, D., Sick, V., "Investigation of the fuel injection, mixing and combustion processes in an SIDI engine using quasi-3D LIF imaging," *SAE Paper* 2003-01-0068, 2003

[16] Amsden, A.A., "KIVA-3V, Release 2, Improvements to KIVA-3V", LA-13608-MS, May 1999

[17] Schmidt, D.P., Nouar, I., Senecal, P.K., Rutland, C.J., Martin, J.K., Reitz, R.D., "Pressure-Swirl Atomization in the Near Field", *SAE Paper* 1999-01-0496, 1999

[18] Senecal, P.K., Schmidt, D.P., Nouar, I., Rutland, C.J., Reitz, R.D., Corradini, M.L., "Modeling High-Speed Viscous Liquid Sheet Atomization", *Int. J. of Multiphase Flow*, 25, pp. 1073-1097, 1999

[19] O'Rourke P.J., Amsden, A.A., "The TAB Method for Numerical Calculation of Spray Droplet Breakup", SAE Technical Paper 872089, 1987

[20] Han, Z., Xu, Z., Trigui, N., "Spray/Wall Interaction Models for Multidimensional Engine Simulation", International Journal of Engine Research 1(1):127-146, 2000